



## Discover Generics

Cost-Effective CT & MRI Contrast Agents



FRESENIUS  
KABI

WATCH VIDEO

# AJNR

## The Oculomotor Cistern: Anatomy and High-Resolution Imaging

K.L. Everton, U.A. Rassner, A.G. Osborn and H.R. Harnsberger

*AJNR Am J Neuroradiol* 2008, 29 (7) 1344-1348

doi: <https://doi.org/10.3174/ajnr.A1089>

<http://www.ajnr.org/content/29/7/1344>

This information is current as of June 23, 2025.

## ORIGINAL RESEARCH

K.L. Everton  
U.A. Rassner  
A.G. Osborn  
H.R. Harnsberger

# The Oculomotor Cistern: Anatomy and High-Resolution Imaging

**BACKGROUND AND PURPOSE:** The oculomotor cistern (OMC) is a small CSF-filled dural cuff that invaginates into the cavernous sinus, surrounding the third cranial nerve (CNIII). It is used by neurosurgeons to mobilize CNIII during cavernous sinus surgery. In this article, we present the OMC imaging spectrum as delineated on 1.5T and 3T MR images and demonstrate its involvement in cavernous sinus pathology.

**MATERIALS AND METHODS:** We examined 78 high-resolution screening MR images of the internal auditory canals (IAC) obtained for sensorineural hearing loss. Cistern length and diameter were measured. Fifty randomly selected whole-brain MR images were evaluated to determine how often the OMC can be visualized on routine scans. Three volunteers underwent dedicated noncontrast high-resolution MR imaging for optimal OMC visualization.

**RESULTS:** One or both OMCs were visualized on 75% of IAC screening studies. The right cistern length averaged  $4.2 \pm 3.2$  mm; the opening diameter (the porus) averaged  $2.2 \pm 0.8$  mm. The maximal length observed was 13.1 mm. The left cistern length averaged  $3.0 \pm 1.7$  mm; the porus diameter averaged  $2.1 \pm 1.0$  mm, with a maximal length of 5.9 mm. The OMC was visualized on 64% of routine axial T2-weighted brain scans.

**CONCLUSION:** The OMC is an important neuroradiologic and surgical landmark, which can be routinely identified on dedicated thin-section high-resolution MR images. It can also be identified on nearly two thirds of standard whole-brain MR images.

The oculomotor nerve (the third cranial nerve [CNIII]) is accompanied by a CSF-filled arachnoid-lined dural cuff as it enters the superolateral cavernous sinus roof. This oculomotor cistern (OMC) is well known to neurosurgeons as an avascular space used to expose and mobilize the nerve during cavernous sinus surgery. However, there has been no radiographic documentation and delineation of this cistern. The OMC is an important landmark for all surgeries involving the roof and lateral walls of the cavernous sinus, the basilar cisterns, the suprasellar area, and the middle cranial base.<sup>1</sup> It is important for radiologists and neurosurgeons planning tumor resection in this area to understand OMC MR imaging anatomy and pathology.

We performed both a retrospective review of routine and high-resolution MR imaging of the brain as well as prospective dedicated imaging of the OMC and the surrounding structures to detail normal OMC imaging anatomy. We also illustrate its appearance in pathology involving the cavernous sinus.

## Materials and Methods

After institutional review board approval, a retrospective review of high-resolution and routine brain MR images and prospective dedicated images of consenting volunteers were used to evaluate the OMC.

Consecutive 1.5T and 3T high-resolution internal auditory canal (IAC) screening studies performed at the University of Utah Hospital

and surrounding clinics during a 1-year period (December 2005 to December 2006) were reviewed. Seventy-eight cases were evaluated with 73 obtained on a 3T Magnetom Trio (Siemens, Erlangen, Germany), 3 obtained on a 1.5T Eclipse (Philips Medical Systems, Best, the Netherlands), and 1 each on 1.5T Magnetom Espree and Avanto (Siemens). In total, seventy-three 3T studies and five 1.5T studies were evaluated. Most high-resolution IAC screening scans were obtained on 3T machines.

Imaging was performed with 3D T2 turbo spin-echo sequences with a 90° flip back pulse on the Siemens scanners (1.5T: TR, 1200 ms; TE, 137 ms; matrix size,  $256 \times 256$ ; section thickness, 0.75 mm; 3T: TR, 750 ms; TE, 110 ms, matrix size,  $268 \times 320$ ; section thickness, 0.8), with a 3D T2 fast spin-echo on the Philips scanner (TR, 3500 ms; TE, 85 ms; matrix size,  $304 \times 512$ ; 0.8-mm section thickness), and with a dual excitation balanced steady-state free precession sequence (bSSFP; on Siemens scanners called constructive interference in steady state [CISS]; 1.5T: TR, 6.7 ms; TE, 3.35 ms; matrix size,  $256 \times 256$ ; section thickness, 0.5 mm; 3T: TR, 5.9 ms; TE, 2.95 ms; matrix size,  $224 \times 256$ ; section thickness, 0.8 mm).

We defined “cisterns” as visualization of an oculomotor nerve that was at least 75% surrounded by dura on T2-weighted coronal images. Porus size was measured as the widest diameter identified at the posterior aspect of the OMC on coronal studies. Cistern length was measured on axial images after determining the OMC porus location by cross-localization from the coronal images.

Fifty consecutive 1.5T and 3T routine whole-brain axial MR images, obtained from December 7, 2006, to December 14, 2006, were also evaluated to determine how often the OMC could be identified.

During the review process, it was found that the OMC was abutted by tumor in 2 separate scans. The pathology was evaluated and confirmed by the authors.

Three volunteers were recruited and informed consent was obtained to undergo noncontrast high-resolution 3T brain MR imaging. Images were acquired on a 3T Magnetom Trio scanner with a dual

Received September 6, 2007; accepted after revision February 6, 2008.

From the Department of Radiology, University of Utah, Salt Lake City, Utah.

Paper previously presented at: 45th Annual Meeting of the American Society of Neuroradiology, June 9–14, 2007; Chicago, Ill.

Please address correspondence to Anne G. Osborn, MD, Department of Radiology, College of Medicine, 1A71 University Hospital, Salt Lake City, Utah 84132; e-mail: Anne.Osborn@hsc.utah.edu

DOI 10.3174/ajnr.A1089

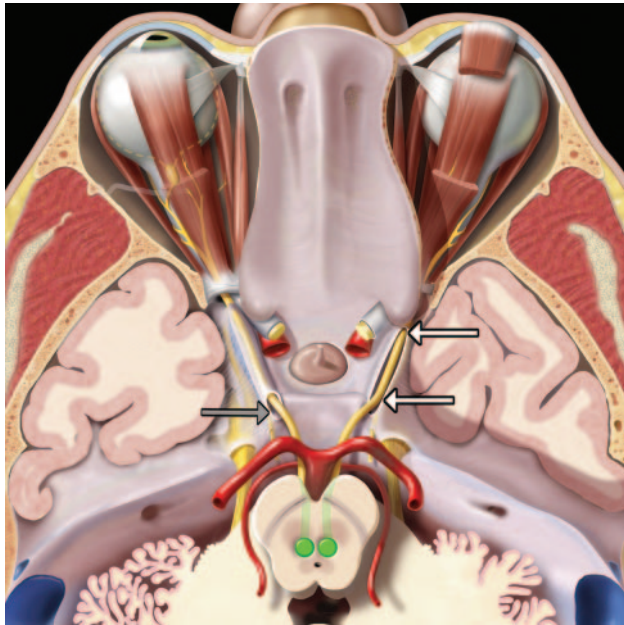


**Fig 1.** An axial graphic of the oculomotor nerves (CN III), seen from above, shows their nuclei (green) in front of the periaqueductal gray matter. Nerve fibers course anteriorly across the red nuclei and substantia nigra and exit the midbrain at the interpeduncular fossa. They then run anterolaterally between the posterior cerebral and superior cerebellar arteries. The nerves enter the cavernous sinus roof at the obliquely oriented porus (gray arrow). Each nerve is accompanied by an arachnoid-lined CSF-filled sleeve (the OMC). The OMC surrounding the right CN III (white arrows) has been opened to depict the nerve as it courses anteriorly within the cistern. The OMCs terminate near the anterior clinoid process as the CN IIIs enter the orbit through the superior orbital fissures.

excitation bSSFP (CISS:  $0.8 \times 0.6 \times 0.6$  mm voxel size; TR, 5.9 ms; TE, 3 ms; flip angle,  $37^\circ$ ). Images were obtained in the axial and coronal planes.

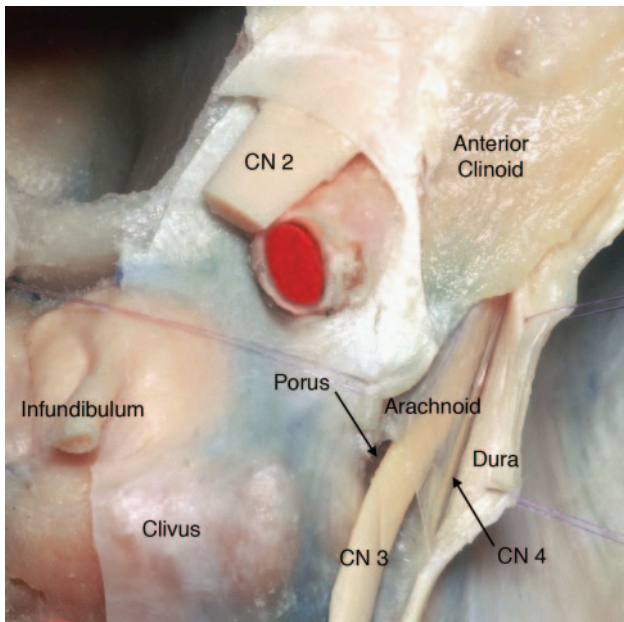


**Fig 2.** Axial anatomic dissection, seen from above, shows the relationship of the right CN III to the clivus and cavernous sinus dura. The dura is dissected and retracted laterally to expose the arachnoid-lined CSF-filled OMC as it runs toward the anterior clinoid. Note the oblique orientation of the porus (modified and reprinted with permission from Martins et al<sup>1</sup>).

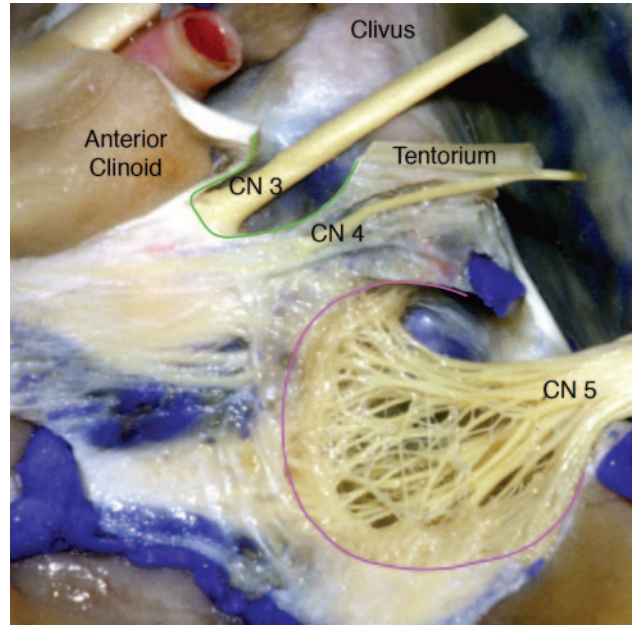


**Fig 3.** Sagittal anatomic dissection of the cavernous sinus with the dura partially removed and the oculomotor nerve exposed. The lateral wall of the OMC has been removed to depict the nerve within the cistern. The OMC is outlined in green. The CN III does not become incorporated into the fibrous dural cavernous sinus wall until it reaches the lower margin of the anterior clinoid process. Meckel cave is outlined in pink (modified and reprinted with permission from Martins et al<sup>1</sup>).

## Results

One or both OMCs were visualized on 75% of high-resolution 1.5T and 3T IAC screening studies. The OMCs were identified on 40% of 1.5T scans (2/5) and 79.5% of 3T scans (58/73). The right cistern averaged  $4.2 \pm 3.2$  mm in length and  $2.2 \pm 0.8$  mm in diameter at its opening (the porus). The maximal length observed was 13.1 mm. The left cistern averaged  $3.0 \pm 1.7$  mm in length and  $2.1 \pm 1.0$  mm in diameter at the porus, with a maximal length of 5.9 mm. The OMC and/or the porus were visualized on 64% of the axial T2-weighted standard 1.5T

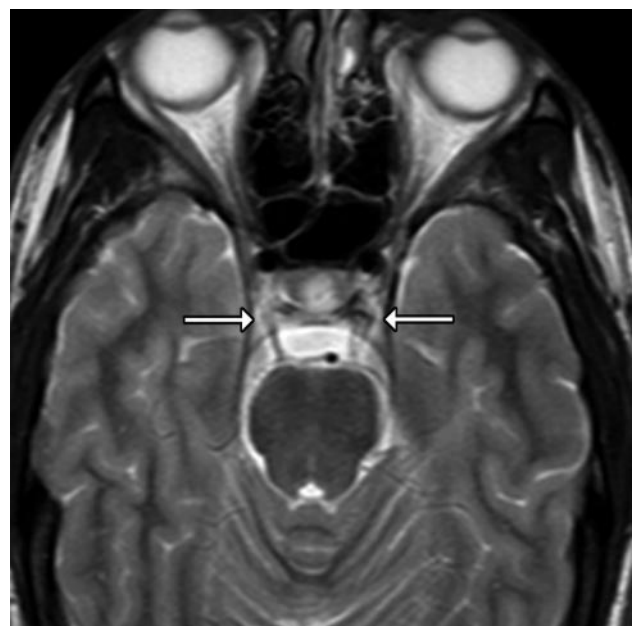


**Fig 4.** Axial T2-weighted image of a routine brain scan shows bilateral OMCs (arrows).

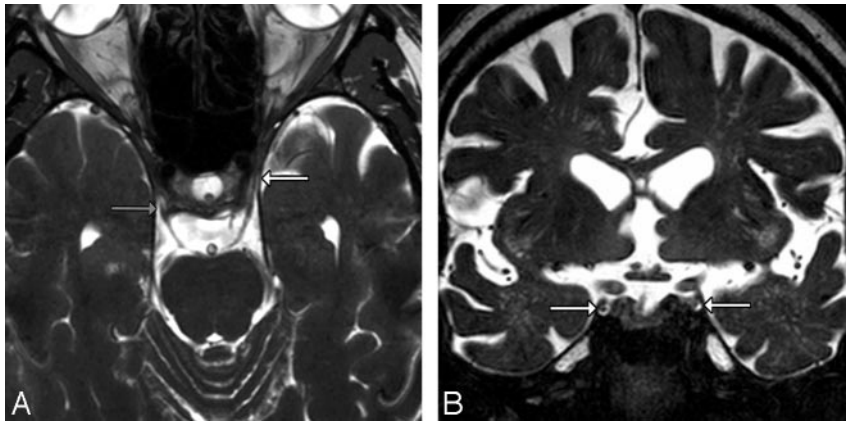


**Fig 5.** A, Axial T2-weighted image from a routine high-resolution 3T screening study to evaluate internal auditory canal lesions shows the right CNIII entering the porus and the left CNIII within the CSF-filled OMC (arrows). B, Coronal T2-weighted image from a routine high-resolution 3T screening study to evaluate IAC lesions shows CNIIIs in the CSF-filled OMCs (arrows).

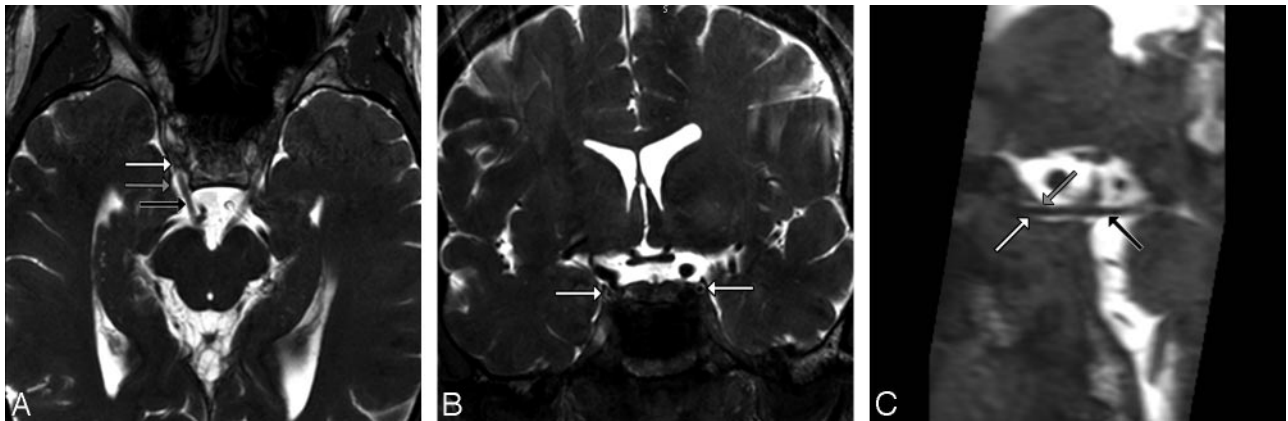


**Fig 6.** A, Dedicated volunteer axial 3T CISS scan shows CNIIIs and OMCs. Note that each nerve (black arrow) enters its OMC through the obliquely oriented porus, seen here as horseshoe-shaped CSF collections (gray arrow) just lateral to the clivus and posterior clinoid processes. Each OMC (white arrow) continues anterolaterally toward the anterior clinoid process. B, Dedicated volunteer coronal 3T CISS scan through the middle of the cavernous sinus shows the CNIIIs within the OMCs. The appearance of isointense "dots" surrounded by hyperintense "rings" of CSF is the most easily identified appearance of the OMC and CNIII (arrows). C, Dedicated volunteer sagittal 3T CISS reformatted from the axial data shows the entire course of CNIII (black arrow) from its exit at the interpeduncular fossa, through the prepontine cistern, and its entrance into the OMC (white arrow) at the porus (gray arrow).

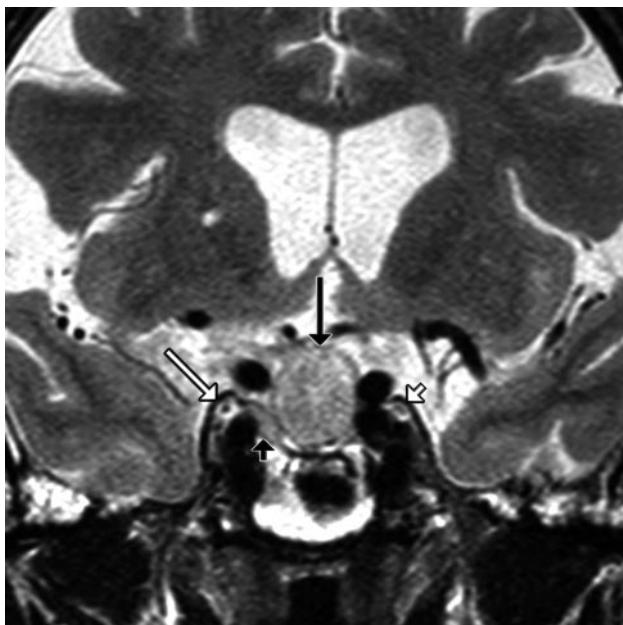


**Fig 7.** Coronal T2-weighted image in a patient with a pituitary macroadenoma (black arrow) shows superolateral extension of the tumor (black arrowhead) toward the CSF-filled OMC (white arrow). Note that the tumor abuts the OMC but does not invade it. The left OMC and CNIII are normal (white arrowhead).

whole-brain scans. The OMC was easily identified on all high-resolution 3T MR imaging volunteer studies. During the review process, it was found that the OMC was invaded by a clival meningioma and abutted by a pituitary microadenoma in 2 separate routine scans. The pathology was evaluated and confirmed by the authors.

## Discussion

The CNIII originates from midbrain nuclei that lie just in front of the periaqueductal gray matter (Fig 1). Its axons course anteriorly through the midbrain, crossing the red nucleus and exiting between the cerebral peduncles at the interpeduncular fossa. After leaving the midbrain, the nerve passes between the posterior cerebral arteries and superior cerebellar arteries. Continuing anteroinferiorly through the interpeduncular fossa, it runs superior and medial to the tentorial edge, just inferolateral to the posterior communicating artery.

The interpeduncular segment of the oculomotor nerve has traditionally been described as terminating when the nerve pierces the lateral aspect of the cavernous sinus and immediately becomes incorporated into its fibrous dural wall. However, detailed surgical dissection shows the interpeduncular segment ends when CNIII enters a variably sized cistern that is filled with CSF and is continuous with the basilar cisterns.<sup>1</sup>

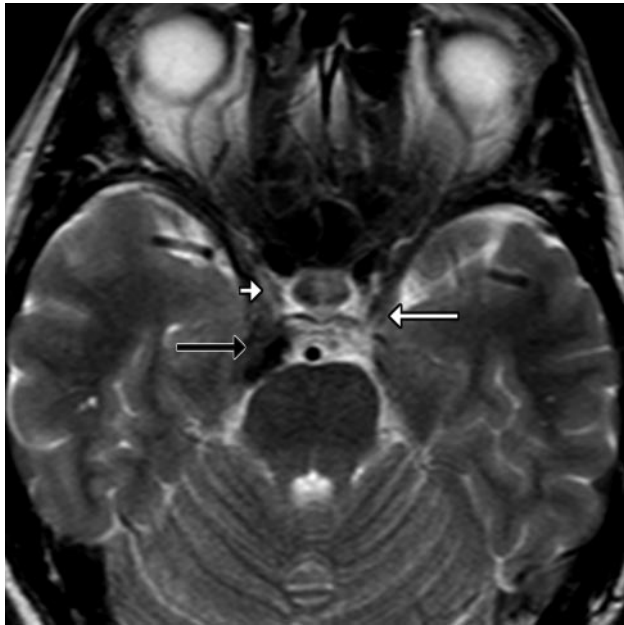


**Fig 8.** Axial T2-weighted image in a patient with diplopia shows the normal CSF-filled OMC surrounding the left third oculomotor nerve (white arrow). An isointense clival meningioma (black arrow) encroaches on the lateral aspect of the right OMC (white arrowhead), effacing the CSF but sparing the third nerve.

The opening of the OMC, located on the roof of the cavernous sinus in the oculomotor triangle, is called the “porus” (Fig 2). After CNIII enters the porus, the OMC surrounds the nerve for a variable distance, gradually tapering and eventually terminating below the tip of the anterior clinoid process (Fig 3).

The intracavernous CNIII has been evaluated extensively from a neurosurgical perspective, and many articles describe the OMC in varying detail.<sup>1-5</sup> The entire CNIII course has also been recently delineated radiologically from its nucleus and tract in the midbrain,<sup>6</sup> across the interpeduncular cistern,<sup>7</sup> through the cavernous sinus,<sup>8</sup> and into the superior orbital fissure and orbital apex.<sup>8,9</sup> Despite numerous descriptions of CNIII in the imaging literature, we found only 2 articles and a textbook that even mention the existence of an OMC.<sup>10-12</sup> Anatomic diagrams in the textbook incorrectly depict the cavernous CNIII segment, and the articles briefly mention—but never identify—the OMC. Some articles that describe intra-

cavernous cranial nerves mention the trigeminal (Meckel cave) and abducens (Dorello canal) cisterns but do not describe the OMC.<sup>13,14</sup> On the other hand, several recent articles actually show the OMC on high-resolution MR images but do not identify the structure.<sup>7-9,15,16</sup>

In an article describing the microsurgical anatomy of the OMC, Martins et al<sup>1</sup> describe dissecting 40 cadavers and were able to identify the cistern in all specimens. Although the OMC could not be identified in 100% of the imaging studies reviewed, two thirds of standard axial whole-brain MR images (Fig 4) and 75% of high-resolution screening 3T MR images clearly showed the OMC (Fig 5). It was not possible to compare high-resolution 1.5T and 3T IAC scans because most scans obtained used 3T MR imaging. The range of porus diameters and cistern lengths was variable, and section thickness may account for some error when looking at specific MR images. In addition, porus measurements may be smaller in diameter on MR imaging scans because coronal scans were not necessarily in plane with the porus. Overall, our measurements were similar to those of the cadaver specimens (width of cistern at porus,  $5.5 \pm 1.1$  mm; length of cistern,  $6.5 \pm 1.5$  mm).<sup>1</sup>

Because the cavernous sinus is such an anatomically complex region and surgical access is difficult, detailed preoperative planning is imperative. The posterior portion of the roof, which contains the oculomotor triangle and the OMC porus, must be opened to allow access to intracavernous tumors or basilar tip aneurysms.<sup>3</sup> Seoane et al<sup>17</sup> described a technique in which the opening of the posterior cavernous sinus roof was initiated by inserting a 90° microdissector into the porus above the nerve and opening the superior wall of the OMC. The OMC thus provides a hydraulic cushion, which also aids in safely exposing the nerve during cavernous sinus surgery.<sup>1</sup>

Using CISS sequences has been described in several articles as an optimal technique to evaluate anatomy that is surrounded by CSF or enhanced cavernous sinus.<sup>7,15,18,19</sup> Because the OMC surrounds CNIII through a large portion of its intracavernous path, we were able to use noncontrast CISS 3T MR imaging to identify the OMC on volunteer scans (Fig 6A–C). However, in most routine brain scans, we found that T2-weighted 1.5T or 3T MR imaging allowed adequate visualization of the cistern and its surrounding structures.



**Fig 9.** A, Coronal T2-weighted image in a patient with generalized dural ectasia shows enlarged OMCs (white arrow), a partial empty sella (black arrow), and patulous Meckel caves (gray arrow). B, Axial T2-weighted image in the same patient shows strikingly enlarged OMCs (arrows). C, A lower section through the IACs shows bilaterally enlarged Meckel caves (white arrows) and Dorello canals (black arrows), part of the generalized dural ectasia. The IACs appear normal.

A recently published neurosurgery case report by Tanriover et al<sup>4</sup> describes a CNIII schwannoma located in the OMC. T1- and T2-weighted MR images show a hypointense mass within the cavernous sinus roof that extends into the superior orbital fissure and shows minimal enhancement. MR angiography demonstrated that the lesion was not of vascular origin. On surgical exploration, the extracavernous (cisternal) portion of CNIII was normal, but the nerve became edematous at the OMC porus. The cavernous sinus roof was opened into the OMC, revealing the tumor. The authors stated that careful evaluation of tumor growth along the cavernous sinus roof and its relationship with the OMC was helpful in preoperative planning and that the OMC may provide a space for CNIII schwannomas to expand in the region of the cavernous sinus.<sup>4</sup>

Castillo<sup>10,12</sup> briefly mentions the OMC in articles describing the upper cranial nerves, and he uses an image illustrating a schwannoma of the intracavernous CNIII, which most likely involved the OMC.

In the evaluation of the OMC by using high-resolution screening MR images, 2 patients were found to have tumors abutting the OMC. One patient had a pituitary microadenoma, which invaded the cavernous sinus and was approaching the OMC (Fig 7). The other patient had a clival meningioma, which invaded the OMC but spared the CNIII (Fig 8). These findings illustrate the importance of oculomotor nerve and cistern anatomy in the evaluation of cavernous sinus pathology and surgical planning.

A third patient showed exaggerated but normal OMCs due to generalized dural ectasia with a partially empty sella, patulous Meckel caves, and easily identified Dorello canals (Fig 9A–C). In this patient, the unusually prominent OMC could be recognized as an otherwise normal structure.

## Conclusion

The OMC can be seen throughout its course from the oculomotor porus on the roof of the cavernous sinus to the inferior surface of the anterior clinoid process. This small dura-arachnoid cuff is filled with CSF and is an important surgical and imaging landmark. The normal OMC should not be mistaken for pathology; rather, it must be recognized as a structure that is highly important to skull base surgeons—a bloodless and relatively safe means to dissect and mobilize CNIII within the cavernous sinus. The OMC may also serve as a potential con-

duit for neoplastic, infectious, microvascular, and inflammatory disorders to invade the cavernous sinus.

## Acknowledgments

We thank Dr. Albert L. Rhoton, Jr. and *Operative Neurosurgery (Op Neurosurg)*. Dr. Rhoton contributed photographs previously published by *Op Neurosurg*. We obtained permission to use these photographs from both parties.

## References

- Martins C, Yasuda A, Campero A, et al. **Microsurgical anatomy of the oculomotor cistern.** *Neurosurgery* 2006;58(4 suppl 2):ONS-220–27, discussion ONS-227–28
- Rhoton A Jr. **The cavernous sinus, the cavernous venous plexus, and the carotid collar.** *Neurosurgery* 2002;51:S375–410
- Yasuda A, Campero A, Martins C, et al. **Microsurgical anatomy and approaches to the cavernous sinus.** *Neurosurgery* 2005;56:4–27
- Tanriover N, Kemerdere R, Kafadar AM, et al. **Oculomotor nerve schwannoma located in the oculomotor cistern.** *Surg Neurol* 2007;67:83–88
- Lu J, Zhu XL. **Characteristics of distribution and configuration of intracranial arachnoid membranes.** *Surg Radiol Anat* 2005;27:472–81
- Yamada K, Shiga K, Kizu O, et al. **Oculomotor nerve palsy evaluated by diffusion-tensor tractography.** *Neuroradiology* 2006;48:434–37
- Yousry I, Camelio S, Schmid UD, et al. **Visualization of cranial nerves I–XII: value of 3D CISS and T2-weighted FSE sequences.** *Eur Radiol* 2000;10:1061–67
- Ettl A, Zwrtek K, Daxer A, et al. **Anatomy of the orbital apex and cavernous sinus on high-resolution magnetic resonance images.** *Surv Ophthalmol* 2000;44:303–23
- Ettl A, Salomonowitz E. **Visualization of the oculomotor cranial nerves by magnetic resonance imaging.** *Strabismus* 2004;12:85–96
- Castillo M. **Imaging of the upper cranial nerves I, III–VIII, and the cavernous sinuses.** *Neuroimaging Clin N Am* 2004;14:579–93
- Harnsberger HR, Osborn AG, Ross J, et al. **Diagnostic and Surgical Imaging Anatomy: Brain, Head and Neck, Spine.** Salt Lake City: Amirsys; 2006:198–99
- Castillo M. **Imaging of the upper cranial nerves I, III–VIII, and the cavernous sinuses.** *Magn Reson Imaging Clin N Am* 2002;10:415–31
- Hermann M, Bobek-Billewicz B, Sloniewski P. **Heavily T2-weighted magnetic resonance landmarks of the cavernous sinus and paracavernous region.** *Skull base Surg* 2000;10:75–80
- Borges A, Casselman J. **Imaging the cranial nerves. Part I. Methodology, infectious and inflammatory, traumatic and congenital lesions.** *Eur Radiol* 2007;17: 2112–25. Epub 2007 Feb 24.
- Held P, Nitz W, Seitz J, et al. **Comparison of 2D and 3D MRI of the optic and oculomotor nerve anatomy.** *Clin Imaging* 2000;24:337–43
- Eisenkraft B, Ortiz AO. **Imaging evaluation of cranial nerves 3, 4, and 6.** *Semin Ultrasound CT MR* 2001;22:488–501
- Seoane E, Tedeschi H, de Oliveira E, et al. **The pretemporal trans cavernous approach to the interpeduncular and prepontine cisterns: microsurgical anatomy and technique application.** *Neurosurgery* 2000;46:891–98
- Seitz J, Held P, Strotzer M, et al. **MR imaging of cranial nerve lesions using six different high-resolution T1- and T2(\*)-weighted 3D and 2D sequences.** *Acta Radiol* 2002;43:349–53
- Yagi A, Sato N, Taketomi A, et al. **Normal cranial nerves in the cavernous sinuses: contrast-enhanced three-dimensional constructive interference in the steady state MR imaging.** *AJNR Am J Neuroradiol* 2005;26:946–50